Muscleblind-Like 1 Knockout Mice Reveal Novel Splicing Defects in the Myotonic Dystrophy Brain

Koichi Suenaga[1,9], Kuang-Yung Lee[2,3,9], Masayuki Nakamori[4,¤a], Yoshiki Tatsumi[1], Masanori P. Takahashi[4], Harutoshi Fujimura[5], Kenji Jinnai[6], Hiroo Yoshikawa[1], Hongqing Du[7,¤b], Manuel Ares Jr.[7], Maurice S. Swanson[2], Takashi Kimura[1]*

1 Division of Neurology, Department of Internal Medicine, Hyogo College of Medicine, Nishinomiya, Hyogo, Japan, 2 Department of Molecular Genetics and Microbiology, College of Medicine, University of Florida, Gainesville, Florida, United States of America, 3 Department of Neurology, Chang Gung Memorial Hospital, Keelung, Taiwan, 4 Department of Neurology, Osaka University Graduate School of Medicine, Suita, Osaka, Japan, 5 Department of Neurology, National Hospital Organization Toneyama Hospital, Toyonaka, Osaka, Japan, 6 Department of Neurology, National Hospital Organization Hyogo-Chuo Hospital, Ohara, Hyogo, Japan, 7 Department of Molecular, Cell and Developmental Biology, RNA Center, Sinsheimer Labs, University of California Santa Cruz, Santa Cruz, California, United States of America

Abstract

Myotonic dystrophy type 1 (DM1) is a multi-systemic disorder caused by a CTG trinucleotide repeat expansion (CTG^{exp}) in the *DMPK* gene. In skeletal muscle, nuclear sequestration of the alternative splicing factor muscleblind-like 1 (MBNL1) explains the majority of the alternative splicing defects observed in the *HSA*^{LR} transgenic mouse model which expresses a pathogenic range CTG^{exp}. In the present study, we addressed the possibility that MBNL1 sequestration by CUG^{exp} RNA also contributes to splicing defects in the mammalian brain. We examined RNA from the brains of homozygous *Mbnl1*$^{\Delta E3/\Delta E3}$ knockout mice using splicing-sensitive microarrays. We used RT-PCR to validate a subset of alternative cassette exons identified by microarray analysis with brain tissues from *Mbnl1*$^{\Delta E3/\Delta E3}$ knockout mice and post-mortem DM1 patients. Surprisingly, splicing-sensitive microarray analysis of *Mbnl1*$^{\Delta E3/\Delta E3}$ brains yielded only 14 candidates for mis-spliced exons. While we confirmed that several of these splicing events are perturbed in both *Mbnl1* knockout and DM1 brains, the extent of splicing mis-regulation in the mouse model was significantly less than observed in DM1. Additionally, several alternative exons, including *Grin1* exon 4, *App* exon 7 and *Mapt* exons 3 and 9, which have previously been reported to be aberrantly spliced in human DM1 brain, were spliced normally in the *Mbnl1* knockout brain. The sequestration of MBNL1 by CUG^{exp} RNA results in some of the aberrant splicing events in the DM1 brain. However, we conclude that other factors, possibly other MBNL proteins, likely contribute to splicing mis-regulation in the DM1 brain.

Introduction

Myotonic dystrophy type1 (DM1) is a multi-systemic disorder affecting skeletal muscle, heart, ocular lens, testis, and the central nervous system (CNS). CNS involvement in adult-onset DM1 includes visual spatial and attention deficits, dysexecutive syndrome, apathy, avoidant behavior and excessive daytime sleepiness (review [1]). Although neuropathological studies have revealed several morphological changes [2,3,4], whether these changes contribute to the clinical symptoms observed in DM1 remains to be determined.

DM1 is caused by the unstable expansion of CTG trinucleotide repeats in the 3′ untranslated region of the DM protein kinase (*DMPK*) gene [5]. Recent evidence suggests that transcripts containing expanded CUG repeats (CUG^{exp}) accumulate in nuclear RNA foci and exert toxic effects on a variety of cellular regulatory pathways including splicing and transcription [6]. One

disease model that is supported by considerable experimental evidence proposes that CUG^{exp} RNAs cause sequestration and inhibition of the RNA-binding protein MBNL1 [7]. In support of this model, *Mbnl1* knockout mice develop the muscle, eye, and RNA splicing abnormalities that are characteristic of DM1 disease [8]. In addition, we have reported a strong correlation in skeletal muscle splicing changes between two mouse models of DM1, the *HSA*^{LR} transgenic and the *Mbnl1* knockout [9].

In the CNS of DM1 patients, mutant *DMPK* transcripts accumulate in neuronal nuclei and sequester MBNL1 and MBNL2 [10]. Although abnormal regulation of several alternatively spliced exons has also been documented in the DM1 brain [10,11,12,13], it is not clear if MBNL1 sequestration contributes to aberrant splicing. Here we used splicing-sensitive microarrays to detect mis-splicing in the *Mbnl1*$^{\Delta E3/\Delta E3}$ knockout brain.

Results

Splicing perturbations in the Mbnl1^ΔE3/ΔE3 knockout brain

To test directly whether loss of MBNL1 expression contributes to aberrant splicing in the CNS, RNA was extracted from the brains of age-matched males carrying homozygous $Mbnl1^{\Delta E3/\Delta E3}$ knockout or wild-type alleles in the same (C57BL/6J) background and analyzed on splicing-sensitive microarrays [9]. Experience with this method indicates that differences in the $\log_2$ of the ratio of exon skipping to inclusion (the skip/include ratio) between two samples (sepscore) with an absolute value >0.3 can be validated by RT-PCR. We observed 14 events in $Mbnl1^{\Delta E3/\Delta E3}$ knockout mice that exceeded this score (Table S1). We used RT-PCR to validate a subset of alternative cassette exons identified by microarray analysis and found four events (Sorbs1 exons 6 and 25, Spag9 exon 31, Dclk1 exon 19) that showed significant differences in splicing between wild-type and knockout mice in both the hippocampus and cerebellum (Figure 1A,B). Sorbs1 is particularly interesting because it is expressed in multiple tissues and exon 25 is regulated during postnatal development [9,14]. In heart, MBNL1 is a major factor which regulates exon 25 splicing with nearly complete inclusion in wild-type adult heart but only ~60% inclusion in the Mbnl1 knockout heart. While this exon is also mis-spliced in the Mbnl1 knockout brain, the effect of MBNL1 loss on this exon is considerably less in both the hippocampus and cerebellum. This modest effect of MBNL1 loss on other mis-regulated exons was also apparent for Spag9 exon 31, Sorbs1 exon 6 and Dclk1 exon 19 (Figure 1B). Nevertheless, these exons are regulated during developmental transition from neonatal (P6) to adult (P42) forebrain (Figure 1A), which indicates other factor may play a role in splicing regulation during this period.

Splicing microarrays also revealed mis-splicing of Camk2d, so we further investigated splicing of this gene. Importantly, Camk2d splicing is regulated during postnatal development with the major isoforms all containing exons 14a and 17 with alternative splicing of the exon 14b, 15 and 16 cassettes to generate several major isoforms, including δ1, δ2, δ3, δ3.1, δ4 and δ9 (Figure 2). Previous reports have indicated that the δ1 isoform is the major splice variant in the adult rat forebrain, while δ4 isoform is expressed in the neonatal rat forebrain [15]. We observed that in P1 whole brain, P6 fore- and hindbrain, δ1 and δ9 are the major isoforms while in adults (P42), exon 15 is preferentially spliced, so that in addition to δ1, δ4 is also the major form in forebrain and both δ4 and δ3 are expressed in hindbrain. In accordance with other splicing changes where immature splicing isoforms are expressed in the adult tissues, splicing of the fetal δ9 isoform significantly increased in the hippocampus of Mbnl1 knockouts compared to controls although the increase was modest and was not observed in the cerebellum. While the δ9 isoform increased, the δ3 (+14b −15 −16) isoform decreased in Mbnl1 knockout mouse hippocampus compared with wild-type.

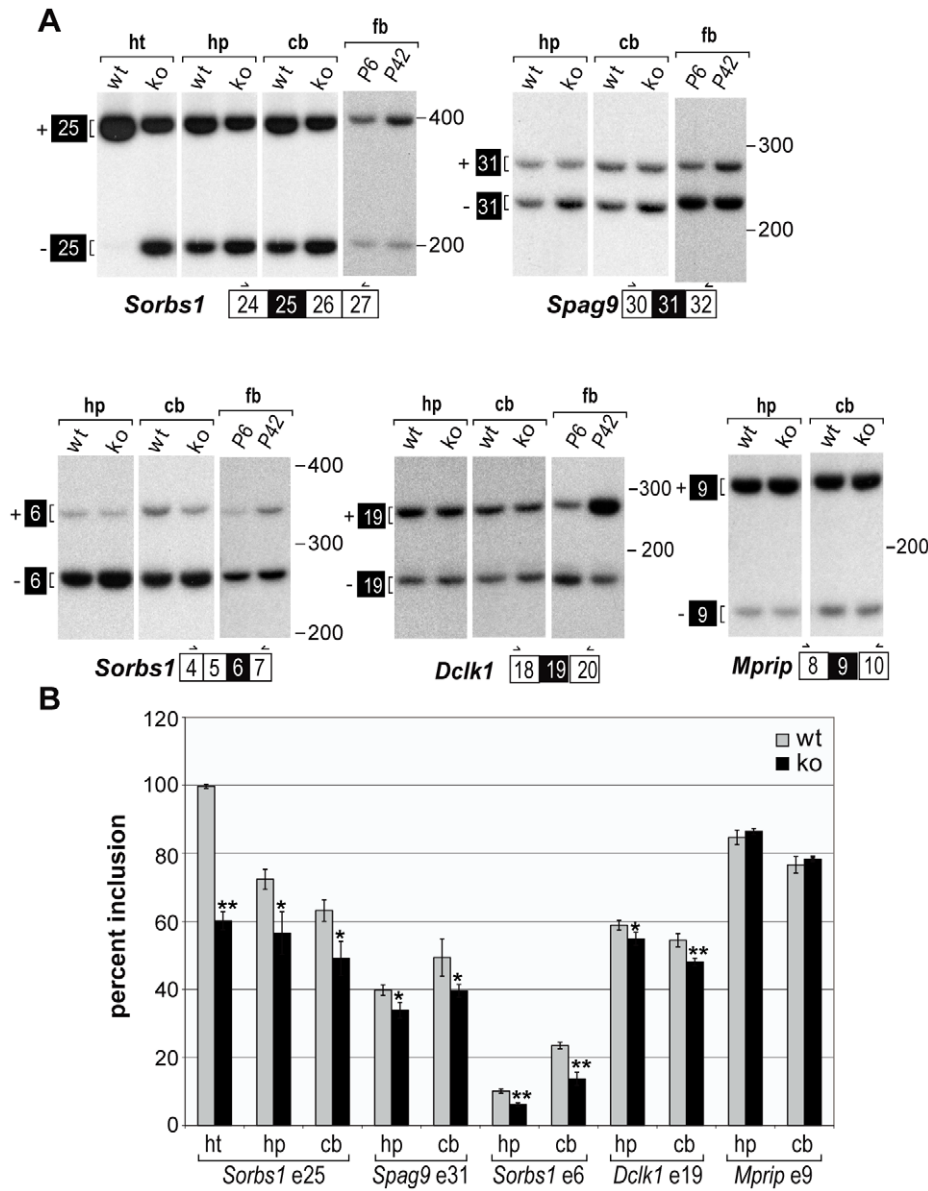## Aberrant splicing in human brain samples and comparison with Mbnl1 knockout brain

To determine whether these mis-splicing events predicted from the Mbnl1 knockout brain microarray data were also observed in the human DM1 brain, we aligned affected mouse exons to the human genome and found 12 exons that are conserved and orthologous to MBNL1-dependent mouse exons (Table S2). We examined all of these events in post-mortem human temporal cortex and cerebellum. The most striking result in human DM1 brain was mis-splicing of SORBS1 exon 26 (orthologous to mouse exon 25). In the temporal cortex, the average percentage of exon

26 inclusion in DM1 was ~40% while those observed in the normal controls and in the disease controls were ~85% and ~90%, respectively (Figure 3A and B, upper). In the cerebellum, exon 26 inclusion was also significantly decreased in DM1 compared with in disease controls, although this difference is subtler than that in the temporal cortex. Both DCLK1 exon 19 inclusion and MPRIP exon 9 inclusion were significantly decreased in DM1 temporal cortex (Figure 3A and B, middle and bottom), whereas there is no difference in these splicing events between DM1 and disease cerebellums.

In humans, the splicing of CAMK2D is also regulated in a tissue-specific and developmental manner. We found that δ9 was expressed almost exclusively in human fetal whole brain (unlike rodent brain), while δ1 was predominantly expressed in adult human temporal cortex samples (Figure 3C to E). In contrast, the percentage of the δ9 isoform was significantly increased in adult DM1 temporal cortex compared to both disease and normal controls. This increase was ~30% in DM1 temporal cortex (Figure 3E), or apparently larger than that observed in the hippocampus of Mbnl1 knockout mice (Figure 2), although we could not conclude which of the following changes will have a stronger impact: (a) an increase from 0 to ~2.5% in Mbnl1 knockout mice (Figure 2C), or (b) an increase from ~10% to ~30% in DM1 temporal cortex (Figure 3E). As a result of the increase of δ9, the percentage of δ1 was significantly decreased in the DM1 temporal cortex. In DM1 and disease control cerebellums, δ9 was a major isoform and there is no difference between these two. Unlike mouse cerebellum, δ3 isoform was not observed in any groups of human brains.

Initially we did temporal lobe autopsy on human since a former report showed splicing defects of several exons in this region [10]. We did hippocampus analysis on mouse because it is a key region of the brain involved in learning and memory. We thought a concern of regional difference between hippocampus and temporal lobe may not be an issue since a report showed similar tau pathology in hippocampus and temporal cortex [4] and we have compared the splicing pattern of each exon in these regions of mouse brain and found similar splicing defects of Sorbs1 exon 25 and Camk2d exon 14–16 (increased expression of δ9) in Mbnl1 knockout mice (Figure S1). We also used cerebellum samples as a reference region since no apparent cerebellar symptoms in DM1 patients and the lack of RNA foci in DM1 cerebellar cortex have been reported [10]. Although we did not show a direct binding of MBNL1 on these RNA by CLIP (cross linked immuno precipitation), we identified several YGCY motifs in the upstream and downstream introns of these alternative spliced cassettes (Table S3).

We determined by Southern blot analysis the CTG repeat number of the same brain tissues from which we took RNA for RT-PCR (Table 1). Cerebral cortex showed greater CTG repeat number and larger intra-tissue CTG length heterogeneities than cerebellum, consistent with a previous observation [16]. The comparison between the degree of aberrant splicing of each exon and each shortest, median and longest CTG repeat number showed no correlation (Figure S2). Several splicing defects have been reported in DM1 brain and we confirmed some of them (exon 4 of GRIN1, exons 3 and 12 of MAPT and exon 9 of APP) in our human DM1 temporal cortex samples (Figure S3A). However, our splicing microarray analysis did not detect any mis-splicing of these exons in the Mbnl1 knockout model. RT-PCR using each set of specific primer for these exons (Grin1 exon 4, Mapt exons 3 and 9, and App exon 7) also revealed no defects of splicing (Figure S3B).
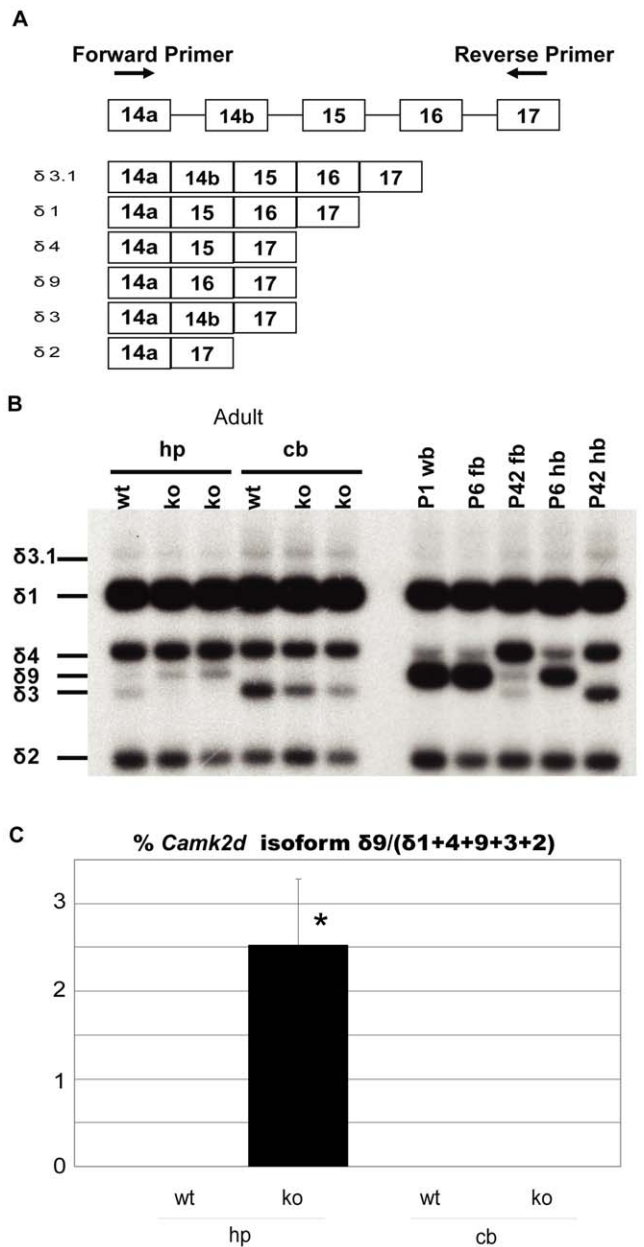
Figure 1. MBNL1 splicing targets in the mouse brain. RT-PCR analysis of wild-type (wt, n = 3, 3–6 months of age) versus Mbnl1$^{\Delta E3/\Delta E3}$ (ko, n = 3, 3–6months of age) brain splicing. (*A*) Representative PCR products. (*B*) Percent exon inclusion measured by phosphoimager analysis. Loss of MBNL1 expression results in reduced exon inclusion for *Sorbs1* exon 25, *Spag9* exon 31, *Sorbs1* exon 6 and *Dclk1* exon 19 in both the hippocampus (hp) and cerebellum (cb). The inclusion of these exons is enhanced in the adult (P42) forebrain (fb) compared to the neonatal (P6) forebrain. *Sorbs1* exon 25 splicing in the heart (ht) and *Mprip* splicing in the brain are included as positive and negative splicing controls. Both unpaired *t*-test and permutation test were used for calculating *p* value (**p* value<0.05, ***p* value<0.01). Averages and standard deviations were generated by unpaired *t*-test.
doi:10.1371/journal.pone.0033218.g001

Discussion

In the present study, we found three novel splicing events, *Sorbs1* exon 25 (exon 26 in human), *Dclk1* exon 19, and *Camk2d* exon 14–16 (exon 14–15 in human), altered both in DM1 and in *Mbnl1* knockout brains. This is the first report of mis-splicing of orthologous exons in brain tissues from human DM1 and *Mbnl1* knockout mice, although mis-splicing of exons 3 and 12 (9 in mice) of *MAPT* has been shown in human DM1 brain [10,13] and in the CTG transgenic mouse brain [17]. In general, the *Mbnl1* knockout hippocampus and DM1 temporal cortex shared similar splicing defects. We also confirmed similar splicing defects of some genes in the hippocampus and temporal cortex of *Mbnl1* knockout mice

(Figure S1). The expression of the fetal splicing isoforms in our samples is consistent with other splicing abnormalities in which fetal splice isoforms are expressed in adult DM1 patients and model mice. Interestingly, only the increase in *GRIN1* exon 4 inclusion in DM1 brain does not represent a return to a fetal splicing profile (Figure S3), which may suggest that distinct splicing factors regulate this splicing event. Our data did not demonstrate directly that MBNL1 regulates the splicing of these exons. However, we found many YGCY motifs that could potentially serve as MBNL1 binding motifs (Table S3) [9].

In human cerebellum, aberrant splicing was less apparent and only splicing of *SORBS1* exon 26 was altered significantly, while similar splicing defects were shown in the hippocampus and
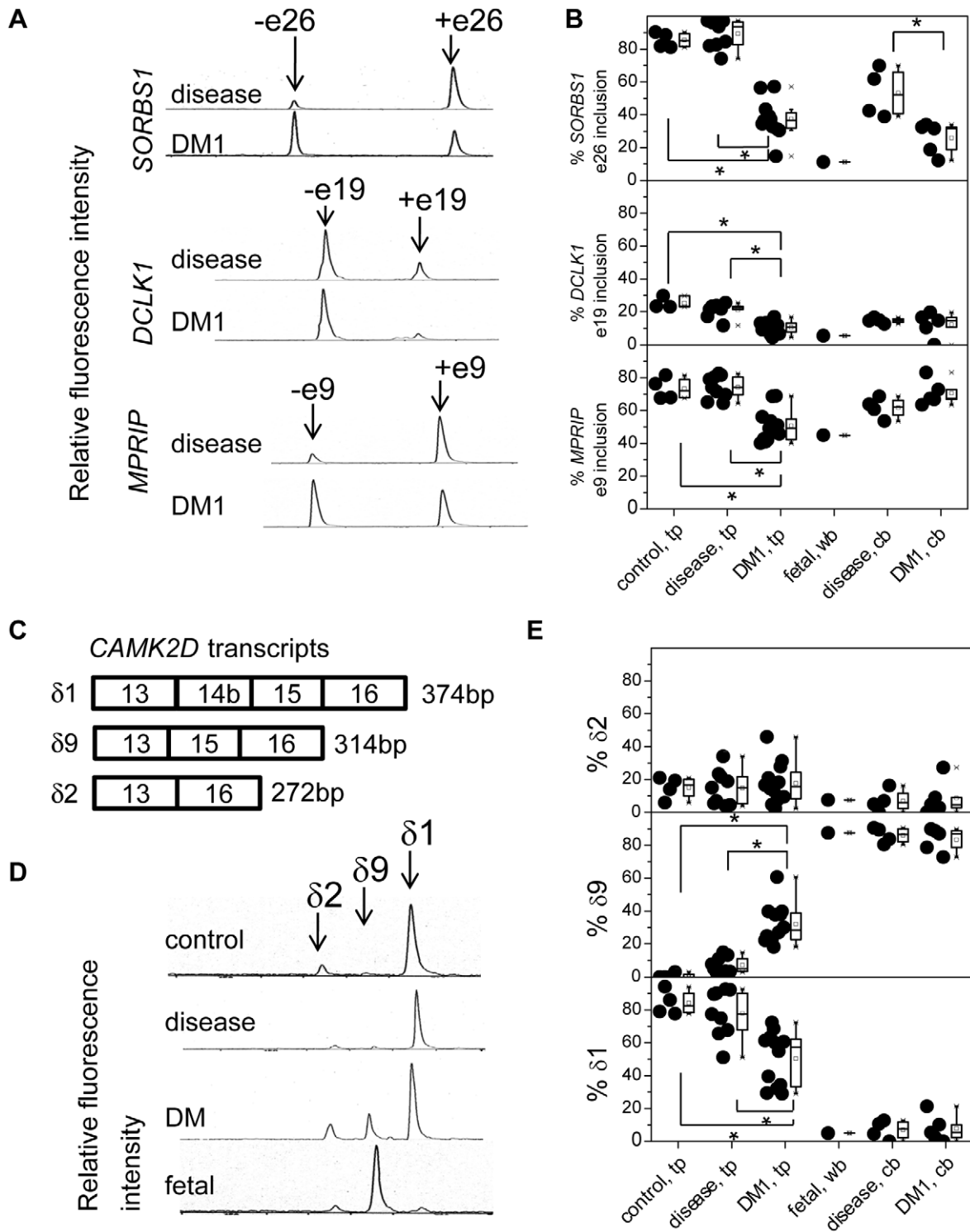
A

Forward Primer   Reverse Primer

| 14a | 14b | 15 | 16 | 17 |

δ3.1 | 14a | 14b | 15 | 16 | 17 |
δ1 | 14a | 15 | 16 | 17 |
δ4 | 14a | 15 | 17 |
δ9 | 14a | 16 | 17 |
δ3 | 14a | 14b | 17 |
δ2 | 14a | 17 |

B

Adult

hp   cb

wt ko ko wt ko ko P1 wb P6 fb P42 fb P6 hb P42 hb

δ3.1

δ1

δ4
δ9
δ3

δ2

C

% Camk2d isoform δ9/(δ1+4+9+3+2)

wt   ko   wt   ko
hp   cb

Figure 2. Spatial and temporal differences in the expression of Camk2d. (A) Transcripts of Camk2d. (B) Representative PCR products. Six spliced isoforms were detected by using primer pairs located in exons 14a and 17. Right panel shows isoform switching from δ9 to δ4 during the fetal (P1, P6) to adult (P42) transition in whole brain (wb), forebrain (fb) and hindbrain (hb) whereas the δ9 isoform was undetectable in adult hindbrain. Left panel shows a detectable increase in the δ9 isoform in Mbnl1$^{\Delta E3/\Delta E3}$ hippocampus (hp) compared with wild-type sibs. However, no δ9 isoform could be detected in the cerebellum of either wild-type or Mbnl1 knockout mice. (C) The percentage of Camk2d isoform δ9 to δ1+4+9+3+2. Both unpaired t-test and permutation test were used for calculating p value (n = 3, *p value<0.05). Averages and standard deviations were generated by unpaired t-test.
doi:10.1371/journal.pone.0033218.g002

cerebellum of the Mbnl1 mouse knockout model. One possible reason for this modest splicing alteration in the cerebellum of human DM1 is that fetal splicing isoforms of some genes are already dominantly expressed in human adult cerebellum and thus

there is no room for any detectable difference of fetal isoforms between DM1 and control samples (e.g. CAMK2D in which fetal δ9 isoform is almost exclusively expressed in both disease control and DM1 cerebellums relative to fetal brain (Figure 3E)). Another possibility is that MBNL1 may not be as efficiently sequestered in RNA foci in the DM1 cerebellar nucleus because the CTG repeat expansion is much smaller in the cerebellum than in the temporal cortex (Table 1). One alternative possibility is that MBNL1 contributes less significantly to the regulation of splicing in human cerebellum. This possibility is unlikely, however, for the following reasons. First, both the immunohistochemistry and western blotting displayed similar expression of MBNL1 in different regions of the brain (Figure S4, Material and Methods S1). Second, since our RT-PCR demonstrated similar splicing defects in Mbnl1 targeted exons in both the hippocampus and cerebellum of Mbnl1 knockout mice (Figure 1), it seems that the contributions of Mbnl1 to these regions are similar.

Compared with Mbnl1 knockout skeletal muscle, where 246 events achieved sepscore values of >0.3 [9], we observed far fewer splicing events that exceeded this score. Some exons previously reported to be mis-spliced in the DM1 brain were not observed in the Mbnl1 knockout brain. In addition, the extent of splicing mis-regulation in the mouse model was significantly less than observed for DM1 (Figures 1, 2, 3). A possible explanation for these smaller splicing changes in Mbnl1 knockout mouse brain is that there are species differences of splicing regulation between mouse and human. However, transgenic mouse brains carrying over 700 CTG repeat have been reported to display splicing abnormalities of Mapt, Grin1, Mbnl1, and Mbnl2 [17]. These results suggest that the contribution of MBNL1 to developmental splicing transitions in the brain is less significant than in skeletal muscle or that the cellular complexity of the brain masks a larger effect of MBNL1 loss on particular cell populations. Three genes encode MBNL paralogs in mammals, MBNL1, MBNL2 and MBNL3, and all of the encoded proteins have been demonstrated to colocalize with nuclear foci in DM1 cells [18]. In reconstruction experiments using transfected cells, each MBNL protein can regulate alternative splicing of pre-mRNAs that are misregulated in DM1 [19]. As MBNL3 is expressed predominantly in the placenta [18], the likely candidate which may play a more significant role in alternative splicing in the brain is MBNL2. While human MBNL1 is expressed primarily in skeletal muscle and heart, MBNL2 is expressed at a similar level in the majority of tissues [18]. Thus, the contribution of MBNL2 to splicing changes may be relatively high in brain in contrast to skeletal muscle. It has been reported that Mbnl1 knockout mice demonstrate cognitive and behavioral abnormalities and normal spatial learning and memory [20]. This relatively mild phenotype may correlate with the modest splicing alteration. Regarding exon 31 of Spag9 and exon 6 of Sorbs1, we found the significant difference between wild-type and Mbnl1 knockout, but not in human brains. This discrepancy may contradict our hypothesis that the recruitment of MBNL1 contributes to the splicing defects in DM1 brains, but may be explained by a difference of splicing regulation between mice and human.

In vitro experiments suggested that a loss of MBNL1 or a gain of CELF1 function could repress exon 3 inclusion but not exon 9 inclusion of Mapt, whereas CELF2 is a repressor of both exons [21]. However, Mbnl1 knockout mice did not show any splicing differences for these exons. This discrepancy about MBNL1 dependent regulation of the splicing of Mapt exon3 between in vitro and mice experiments may also indicate that some redundant factors function in this splicing regulation and loss of MBNL1

Figure 3. Aberrant splicing events in *Mbnl1*[ΔE3/ΔE3] brain are also observed in the human DM1 brain. We compared brain RNA from normal control temporal cortex (control, tp, n = 4), disease control temporal cortex (disease, tp, n = 9), myotonic dystrophy type 1 temporal cortex (DM1, tp, n = 12), fetal control whole brain (fetal, wb, n = 1), disease control cerebellum (disease, cb, n = 4), and DM1 cerebellum (DM1, cb, n = 5). (A) Representative RT-PCR products detected with microchip electrophoretic separation using SV1210 software on the Hitachi SV1210 from exclusion and inclusion of exon 26 of *SORBS1* (upper), exon 19 of *DCLK1* (middle), and exon 9 of *MPRIP* (bottom). (B) Graphical representation of RT-PCR analysis depicting percentages of exon 26 inclusion of *SORBS1* (upper), exon 19 inclusion of *DCLK1* (middle), and exon 9 inclusion of *MPRIP* (bottom). (C) Transcripts of *CAMK2D*. (D) Representative RT-PCR products from *CAMK2D* isoforms: δ2(−exon14b−exon15), δ9(−exon14b+exon15), and δ1(+exon14b+exon15) indicated by each arrow. (E) Graphical representation of RT-PCR analysis depicting percentages of δ2 (upper), δ9 (middle) and δ1 (bottom). Mann-Whitney U test was used for calculating the *p* value. Statistically significant differences (*p*<0.05) are indicated by an asterisk.
doi:10.1371/journal.pone.0033218.g003

Table 1. Human samples analysed.

Patient no/sex	Age	disaese	Sources	CTG repeats in brain samples
C1/M	23	[a]normal	temporal cortex	
C2/M	22	[a]normal	temporal cortex	
C3/M	26	[a]normal	temporal cortex	
C4/F	78	[b]normal	temporal cortex	
D1/F	69	PD	temporal cortex	
D2/F	84	MSA-C	temporal cortex	
D3/F	80	ALS	temporal cortex	
D4/M	53	ALS	temporal cortex	
			cerebellum	
D5/F	81	ALS	temporal cortex	
			cerebellum	
D6/M	70	ALS	temporal cortex	
D7/F	75	ALS	temporal cortex	
D8/F	61	ALS	temporal cortex	
			cerebellum	
D9/M	70	ALS	temporal cortex	
			cerebellum	
DM1/M	58	DM1	temporal cortex	3000–6000
DM2/M	69	DM1	temporal cortex	3000–6000
DM3/M	50	DM1	temporal cortex	2000–6000
DM4/F	56	DM1	temporal cortex	3000–5000
			cerebellum	400
DM5/M	63	DM1	temporal cortex	1200–3000
DM6/M	59	DM1	temporal cortex	3000–9000
DM7/F	58	DM1	temporal cortex	3000–6000
			cerebellum	2200–3000
DM8/F	58	DM1	temporal cortex	2000–8000
DM9/F	58	DM1	temporal cortex	2200–6500
			cerebellum	300
DM10/F	66	DM1	temporal cortex	1900–3300
			cerebellum	150
DM11/M	64	DM1	temporal cortex	2400–5200
DM12/F	73	DM1	temporal cortex	1900–4800
			cerebellum	200
F1/F	21w	[c]fetal	whole brain	

[a]from Biochain,
[b]from Ambion,
[c]from Stratagene, PD; Parkinson's disease; MSA-C; multiple system atrophy with predominant cerebellar ataxia; ALS: amyotrophic lateral sclerosis.
doi:10.1371/journal.pone.0033218.t001

alone is insufficient to change the splicing pattern of this exon in the brain.

SORBS1 was identified as a Cbl-associated protein likely to participate in insulin signaling [22]. The targeted exon encodes the nuclear localization sequence (NLS) [23], suggesting that the protein without an NLS is increased in the DM1 brain and might not be able to function as a nuclear protein. Among the four types of CAMK2 isoforms, the CAMK2D is expressed predominantly in the suprachiasmatic nucleus, substantia nigra, and striatum in the brain. Since each spliced isoform of CAMK2D has been reported to show a distinct distribution pattern [24,25], the increase in δ9

might cause abnormal localization. Interestingly, CAMK2D has been reported to play an essential role in PER1 expression, which is possibly involved in light-induced phase shifts [26]. Although excessive daytime sleepiness and dysregulation of REM sleep occur frequently in patients with DM1, it was reported that the pathophysiologic basis is distinct from narcolepsy, as patients with DM1 do not have a consistent defect of hypocretin release or receptor splicing [27]. Possibly, aberrant splicing of *CAMK2D* might be associated with excessive daytime sleepiness in DM1. DCLK1 is a microtubule-associated kinase that can undergo autophosphorylation and regulate microtubule polymerization [28]. The fetus specific C-terminal splicing variant (exon 19 exclusion), which is expressed more in DM1 adult temporal cortex, showed enhanced autophosphorylation activity and has been suggested a possible role in migrating neurons [29]. Therefore, the increase in the fetal variant of DCLK1 in DM1 brain may cause an abnormal neuronal migration. MPRIP was initially identified as an 116 kDa protein that interacts with RhoA [30]. In neuronal cells, MPRIP is essential for neurite outgrowth and may act as a scaffold to target the myosin phosphatase complex to the actin cytoskeleton [31]. Although the difference between splicing isoforms has not been reported, aberrant splicing of this gene could give rise to abnormal neurite outgrowth in DM1 brain.

In this study, we detected three novel splicing targets which were mis-regulated in both *Mbnl1* knockout mice and human DM1, two only in *Mbnl1* knockout mice, and one only in human DM1 brains. Since the brain is a heterogeneous organ consisting of many different cell types, splicing events may be regulated in a region-specific manner. Our studies support this interpretation with distinct variations in the splicing of developmentally-regulated exons observed in the hippocampus and cerebellum. Our results suggest that at least some of the aberrant splicing events in the DM1 brain result from the sequestration of MBNL1 by CUG^{exp} RNAs. Additionally, it is also likely that other RNA-associated proteins contribute to the aberrant splicing in DM1. Thus, it will be important to investigate the splicing targets in brain samples derived from other DM1 model mice, including *Celf1* transgenic, *Celf2* transgenic and *Mbnl2* knockout mice.

Materials and Methods

Ethics Statement

All experiments using mice were performed in accordance with the guidelines of the University of Florida. The protocol was approved by the University of Florida Institutional Animal Care and Use Committee (Permit Number: #200903677). All experiments using human samples were approved by the Ethics Committee of Hyogo College of Medicine (Permit number: 93) and written informed consent for specimen use for research was obtained from all patients.

Splicing Microarray Detection

RNA samples from the brain of individual 12–14-week-old male mice from the wild-type and *Mbnl1*$^{\Delta E3/\Delta E3}$ lines (n = 4 for each group) were compared. To identify MBNL1-dependent splicing events, RNA from *Mbnl1*$^{\Delta E3/\Delta E3}$ mice was compared to wild-type mice in the C57BL/6J (N10) background. RNA samples were processed for cDNA synthesis and hybridization to Affymetrix "A-chip" oligonucleotide microarrays as follows. Total RNA was primed with random hexamers and reverse transcribed. After the reaction was completed, RNA was removed from the reaction by alkaline hydrolysis and the cDNA was purified using Qiagen PCR Quick Purification Kit. A typical reaction started with 5 μg of total RNA usually yielded ~3 μg of cDNA. The cDNA was then

fragmented using DNase I in an empirically controlled reaction that yields DNA fragments of 50–200 bases. This fragmented cDNA was then end labeled using terminal deoxynucleotidyl transferase and "DNA-Labeling-Reagent-1a (DLR-1a)", which is a biotinylated dideoxynucleoside triphosphate. Labeled cDNA was hybridized to arrays in standard Affymetrix hybridization buffer for 16 hrs at 50°C. Arrays were washed, processed with anti-biotin antibodies and streptavidin-phycoerythrin according to the standard Affymetrix protocol.

Microarray Data Analysis

Analysis was done according to Sugnet et al. [32], who calculate a "separation score" that measures the relative change in ratio of alternative splicing events. The equation for sepscore is:

$$\text{Separation score (sepscore)} =$$

$$\text{Log}_2[\text{mut(skip/include)}/\text{wt(skip/include)}]$$

For each replicate set (each tissue from $Mbnl1^{\Delta E3/\Delta E3}$ and wild type), we estimated the $\log_2$ ratio of skipping to inclusion using robust least squares analysis. We evaluated sepscore significance by permuting the assignments of data points to replicate sets, calculating the separation score for the permuted data, and estimating the likelihood that the observed data came from the permuted distribution. The microarray data have been deposited in NCBI's Gene Expression Omnibus and are accessible through GEO series accession number GSE28640 (http://www.ncbi.nlm. nih.gov/geo/query/acc.cgi?acc=GSE28640). All data is MIAME compliant and the raw data has been deposited in a MIAME compliant database (GEO), as detailed on the MGED Society website (http://www.mged.org/Workgroups/MIAME/miame. html).

Target validation by RT-PCR for model mice

The sequences of primers used for RT–PCR assays of splicing in mouse and human brain RNA are listed in (Tables S1 and S2). To test mouse MBNL1 potential splicing targets identified by splicing microarrays, we harvested hippocampal, temporal cortex and cerebellar tissues from $Mbnl1^{+/+}$ (n = 3) and $Mbnl1^{\Delta E3/\Delta E3}$ (n = 3) mice (C57BL/6J background) ranging from 3–6 months of age. RNA was isolated using TRI Reagent (Sigma) and cDNA generated using 5 μg of RNA, oligo (dT)$_{20}$ (Invitrogen) and SuperScript III (Invitrogen) followed by digestion with 0.2 units/μl RNase H (Invitrogen) at 37°C for 20 min. Splicing targets with predicted alternately spliced cassettes were selected from microarray list and 5 ng of cDNA was PCR-amplified for 28 cycles (95°C for 30 sec, 55°C for 30 sec, 72°C for 30 sec) by using forward and reverse primers located in the flanking exons. Each PCR reaction was spiked with 2.5 μCi of [α^{32}P]-dCTP (PerkinElmer Life Sciences). PCR products were resolved on 10% nondenaturing polyacrylamide gels followed by autoradiography using Kodak BioMax MS film (PerkinElmer Life Sciences). Exon inclusion was measured using a Typhoon 9200 imager and ImageQuant TL software (GE Healthcare).

RT-PCR and Southern blot analysis for human brain samples

Human temporal cortex and cerebellar tissues (n = 21) at autopsy were analyzed (Table 1). RNA was extracted from each sample by the ISOGEN procedure (Nippon Gene). The RNAs used as normal controls were purchased commercially as follows: human adult temporal cortex (3 male, 1female, 3 samples from Biochain, 1 sample from Ambion) and 1 sample of human fetal

whole brain (Stratagene) (Table 1). The quality of RNA and the PCR product were analyzed by capillary electrophoresis using a Hitachi SV 1210 on a microchip (Hitachi Electronics Co., Tokyo, Japan) [33]. We used the samples which meet the criteria that the ratio of 28S/18S rRNA peaks was >0.8. The CTG trinucleotide repeat expansion sizes of human brain samples were determined by Southern blot analysis of genomic DNAs from each brain region tissue of DM1 as described previously [34]. cDNA was synthesized using the same method as for mouse samples except 1–3 μg of RNA and random hexamers were used. cDNA equivalent to 20 ng RNA was PCR-amplified for initial denaturation at 94°C for 10 min and 35 cycles (94°C for 30 sec, 55°C for 30 sec, 72°C for 30 sec) by using forward and reverse primers located in the exons adjacent to the human exons orthologous to mouse exons predicted by the microarray data (Table S2). We determined the percentage of each peak by dividing each signal by the total signal.

Statistical analysis

Differences for the levels of exon inclusion for age-matched genetically homogeneous mice were analyzed by unpaired t- and permutation tests. The data for human samples were analyzed using the nonparametric Mann-Whitney U test because the backgrounds such as age and CTG repeat number of each sample are regarded inhomogeneous and the data for these samples were not always normally distributed.

Supporting Information

Figure S1 *Sorbs1* **exon 25 inclusion is decreased and** *Camk2d* **δ9 is increased to similar extent in the hippocampus (hp) and temporal cortex (tp) of** $Mbnl1^{\Delta E3/\Delta E3}$ **(ko) mice compared with wild type (wt) mice.**
(TIF)

Figure S2 **Comparison between the degree of aberrant splicing and CTG repeat number in DM1 brain.** There was no significant correlation between each shortest, median and longest CTG repeat number, and percent inclusion of each of the exons which are mis-regulated. (A) Temporal tissues. (B) Cerebellar tissues. Spearman rank correlation coefficient was used for the analysis of correlation.
(TIF)

Figure S3 **Some splicing defects which have been reported in DM1 brain were not reproduced in** *Mbnl1* **knockout brain.** (A) Four splicing exons are mis-regulated in our human DM1 temporal cortex (exon4 of *GRIN1*, exons 3 and 12 of *MAPT*, and exon9 of *APP*). Mann-Whitney U test was used for calculating the p value. Statistically significant differences ($p<0.05$) are indicated by an asterisk. (B) These exons are normally spliced in the hippocampus (hp) of *Mbnl1* knockout mice.
(TIF)

Figure S4 **MBNL1 distribution and expression in regions of mouse brain.** (A) Immunohistochemistry with anti-MBNL1 antibody shows that MBNL1 is ubiquitously expressed in the frontal cortex (top), hippocampus (middle), and cerebellum (bottom) sections from wild-type (wt, right) but not in those from *Mbnl1* knockout (ko, left). (B) Western blot analysis shows a similar expression of MBNL1 in the cerebellum, temporal cortex, and hippocampus of a wild-type mouse. (Materials and Methods S1).
(TIF)

Materials and Methods S1 **Supplementary Materials and Methods for Muscleblind-Like 1 Knockout Mice**

Reveal Novel Splicing Defects in the Myotonic Dystrophy Brain.
(DOC)

Table S1   Separation score and primers for RT-PCR of mouse brain.
(DOC)

Table S2   Primers for RT-PCR of human brain.
(DOC)

Table S3   YGCY motif searching list with sequences exons aberrantly regulated in brains of *Mbnl1* knockout mice and DM1 patients. YGCY motifs are indicated by capitals.
(DOC)

Author Contributions

Conceived and designed the experiments: KS K-YL HF KJ MA MSS TK. Performed the experiments: KS K-YL MN YT HF KJ HD MSS. Analyzed the data: KS MN YT MPT KJ HY HD MA MSS TK. Contributed reagents/materials/analysis tools: HF KJ. Wrote the paper: KS K-YL MN YT MPT HY MA MSS TK.

References

1. Meola G, Sansone V (2007) Cerebral involvement in myotonic dystrophies. Muscle Nerve 36: 294–306.
2. Ono S, Kanda F, Takahashi K, Fukuoka Y, Jinnai K, et al. (1996) Neuronal loss in the medullary reticular formation in myotonic dystrophy: a clinicopathological study. Neurology 46: 228–231.
3. Ono S, Inoue K, Mannen T, Mitake S, Shirai T, et al. (1989) Intracytoplasmic inclusion bodies of the thalamus and the substantia nigra, and Marinesco bodies in myotonic dystrophy: a quantitative morphological study. Acta neuropathol 77: 350–356.
4. Vermersch P, Sergeant N, Ruchoux MM, Hofmann-Radvanyi H, Wattez A, et al. (1996) Specific tau variants in the brains of patients with myotonic dystrophy. Neurology 47: 711–717.
5. Harper PS (2001) Myotonic Dystrophy 3rd ed. W. B. Saunders.
6. Sicot G, Gourdon G, Gomes-Pereira M (2011) Myotonic dystrophy, when simple repeats reveal complex pathogenic entities: new findings and future challenges. Hum Mol Genet 20: R116–123.
7. Mankodi A, Logigian E, Callahan L, McClain C, White R, et al. (2000) Myotonic dystrophy in transgenic mice expressing an expanded CUG repeat. Science 289: 1769–1773.
8. Kanadia RN, Johnstone KA, Mankodi A, Lungu C, Thornton CA, et al. (2003) A muscleblind knockout model for myotonic dystrophy. Science 302: 1978–1980.
9. Du H, Cline MS, Osborne RJ, Tuttle DL, Clark TA, et al. (2010) Aberrant alternative splicing and extracellular matrix gene expression in mouse models of myotonic dystrophy. Nat Struct Mol Biol 17: 187–193.
10. Jiang H, Mankodi A, Swanson MS, Moxley RT, Thornton CA (2004) Myotonic dystrophy type 1 is associated with nuclear foci of mutant RNA, sequestration of muscleblind proteins and deregulated alternative splicing in neurons. Hum Mol Genet 13: 3079–3088.
11. Dhaenens CM, Schraen-Maschke S, Tran H, Vingtdeux V, Ghanem D, et al. (2008) Overexpression of MBNL1 fetal isoforms and modified splicing of Tau in the DM1 brain: Two individual consequences of CUG trinucleotide repeats. Exp Neurol 210: 467–478.
12. Leroy O, Wang J, Maurage CA, Parent M, Cooper T, et al. (2006) Brain-specific change in alternative splicing of Tau exon 6 in myotonic dystrophy type 1. Biochim Biophys Acta 1762: 460–467.
13. Sergeant N, Sablonniere B, Schraen-Maschke S, Ghestem A, Maurage CA, et al. (2001) Dysregulation of human brain microtubule-associated tau mRNA maturation in myotonic dystrophy type 1. Hum Mol Genet 10: 2143–2155.
14. Kalsotra A, Xiao X, Ward AJ, Castle JC, Johnson JM, et al. (2008) A postnatal switch of CELF and MBNL proteins reprograms alternative splicing in the developing heart. Proc Natl Acad Sci U S A 105: 20333–20338.
15. Donai H, Murakami T, Amano T, Sogawa Y, Yamauchi T (2000) Induction and alternative splicing of delta isoform of Ca(2+)/calmodulin-dependent protein kinase II during neural differentiation of P19 embryonal carcinoma cells and during brain development. Brain Res Mol Brain Res 85: 189–199.
16. Lopez Castel A, Nakamori M, Tome S, Chitayat D, Gourdon G, et al. (2011) Expanded CTG repeat demarcates a boundary for abnormal CpG methylation in myotonic dystrophy patient tissues. Hum Mol Genet 20: 1–15.
17. Gomes-Pereira M, Foiry L, Nicole A, Huguet A, Junien C, et al. (2007) CTG trinucleotide repeat "big jumps": large expansions, small mice. PLoS Genet 3: e52.
18. Fardaei M, Rogers MT, Thorpe HM, Larkin K, Hamshere MG, et al. (2002) Three proteins, MBNL, MBLL and MBXL, co-localize in vivo with nuclear foci of expanded-repeat transcripts in DM1 and DM2 cells. Hum Mol Genet 11: 805–814.
19. Ho TH, Charlet BN, Poulos MG, Singh G, Swanson MS, et al. (2004) Muscleblind proteins regulate alternative splicing. EMBO J 23: 3103–3112.
20. Matynia A, Ng CH, Dansithong W, Chiang A, Silva AJ, et al. (2010) Muscleblind1, but not Dmpk or Six5, contributes to a complex phenotype of muscular and motivational deficits in mouse models of myotonic dystrophy. PLoS One 5: e9857.
21. Dhaenens CM, Tran H, Frandemiche ML, Carpentier C, Schraen-Maschke S, et al. (2011) Mis-splicing of Tau exon 10 in myotonic dystrophy type I is reproduced by overexpression of CELF2 but not by MBNL1 silencing. Biochim Biophys Acta 1812: 732–742.
22. Ribon V, Printen JA, Hoffman NG, Kay BK, Saltiel AR (1998) A novel, multifuntional c-Cbl binding protein in insulin receptor signaling in 3T3-L1 adipocytes. Mol Cell Biol 18: 872–879.
23. Lebre AS, Jamot L, Takahashi J, Spassky N, Leprince C, et al. (2001) Ataxin-7 interacts with a Cbl-associated protein that it recruits into neuronal intranuclear inclusions. Hum Mol Genet 10: 1201–1213.
24. Xu X, Yang D, Ding JH, Wang W, Chu PH, et al. (2005) ASF/SF2-regulated CaMKIIdelta alternative splicing temporally reprograms excitation-contraction coupling in cardiac muscle. Cell 120: 59–72.
25. Takeuchi Y, Nomura K, Fukunaga K (2004) Differential subcellular distribution of Ca2+/calmodulin-dependent protein kinase II isoforms in the striatum and NG108-15 cells. J Neurosci Res 75: 480–490.
26. Nomura K, Takeuchi Y, Yamaguchi S, Okamura H, Fukunaga K (2003) Involvement of calcium/calmodulin-dependent protein kinase II in the induction of mPer1. J Neurosci Res 72: 384–392.
27. Ciafaloni E, Mignot E, Sansone V, Hilbert JE, Lin L, et al. (2008) The hypocretin neurotransmission system in myotonic dystrophy type 1. Neurology 70: 226–230.
28. Lin PT, Gleeson JG, Corbo JC, Flanagan L, Walsh CA (2000) DCAMKL1 encodes a protein kinase with homology to doublecortin that regulates microtubule polymerization. J Neurosci 20: 9152–9161.
29. Burgess HA, Reiner O (2002) Alternative splice variants of doublecortin-like kinase are differentially expressed and have different kinase activities. J Biol Chem 277: 17696–17705.
30. Gebbink MF, Kranenburg O, Poland M, van Horck FP, Houssa B, et al. (1997) Identification of a novel, putative Rho-specific GDP/GTP exchange factor and a RhoA-binding protein: control of neuronal morphology. J Cell Biol 137: 1603–1613.
31. Mulder J, Ariaens A, van den Boomen D, Moolenaar WH (2004) p116Rip targets myosin phosphatase to the actin cytoskeleton and is essential for RhoA/ROCK-regulated neuritogenesis. Mol Biol Cell 15: 5516–5527.
32. Sugnet CW, Srinivasan K, Clark TA, O'Brien G, Cline MS, et al. (2006) Unusual intron conservation near tissue-regulated exons found by splicing microarrays. PLoS Comput Biol 2: e4.
33. Kataoka M, Inoue S, Kajimoto K, Sinohara Y, Baba Y (2004) Usefulness of microchip electrophoresis for reliable analyses of nonstandard DNA samples and subsequent on-chip enzymatic digestion. Eur J Biochem 271: 2241–2247.
34. The International Myotonic Dystrophy Consortium (IDMC). (2000) New nomenclature and DNA testing guidelines for myotonic dystrophy type 1 (DM1). Neurology 54: 1218–1221.